

Article

# High Resolution Orthomosaics of African Coral Reefs: A Tool for Wide-Scale Benthic Monitoring

Marco Palma <sup>1,†</sup> , Monica Rivas Casado <sup>2,\*</sup> , Ubaldo Pantaleo <sup>1,3</sup> and Carlo Cerrano <sup>1</sup> 

<sup>1</sup> Dipartimento di Scienze della Vita e dell'Ambiente (DISVA), Via Breccie Bianche, Monte Dago,

60130 Ancona, Italy; m.palma@pm.univpm.it (M.P.); info@ubicasrl.com (U.P.); c.cerrano@univpm.it (C.C.)

<sup>2</sup> Cranfield Institute for Resilient Futures, School of Water, Energy and Environment, Cranfield University, Cranfield MK430AL, UK

<sup>3</sup> UBICA srl (Underwater Bio-Cartography), Via San Siro 6/1, 16124 Genova, Italy

\* Correspondence: m.rivas-casado@cranfield.ac.uk; Tel.: +44-(0)-1234-750-111

† Cranfield Institute for Resilient Futures, School of Water, Energy and Environment, Cranfield University, Cranfield MK430AL, UK

Academic Editors: Stuart Phinn and Xiaofeng Li

Received: 27 March 2017; Accepted: 4 July 2017; Published: 8 July 2017

**Abstract:** Coral reefs play a key role in coastal protection and habitat provision. They are also well known for their recreational value. Attempts to protect these ecosystems have not successfully stopped large-scale degradation. Significant efforts have been made by government and research organizations to ensure that coral reefs are monitored systematically to gain a deeper understanding of the causes, the effects and the extent of threats affecting coral reefs. However, further research is needed to fully understand the importance that sampling design has on coral reef characterization and assessment. This study examines the effect that sampling design has on the estimation of seascape metrics when coupling semi-autonomous underwater vehicles, structure-from-motion photogrammetry techniques and high resolution (0.4 cm) underwater imagery. For this purpose, we use FRAGSTATS v4 to estimate key seascape metrics that enable quantification of the area, density, edge, shape, contagion, interspersion and diversity of sessile organisms for a range of sampling scales (0.5 m × 0.5 m, 2 m × 2 m, 5 m × 5 m, 7 m × 7 m), quadrat densities (from 1–100 quadrats) and sampling strategies (nested vs. random) within a 1655 m<sup>2</sup> case study area in Ponta do Ouro Partial Marine Reserve (Mozambique). Results show that the benthic community is rather disaggregated within a rocky matrix; the embedded patches frequently have a small size and a regular shape; and the population is highly represented by soft corals. The genus *Acropora* is the more frequent and shows bigger colonies in the group of hard corals. Each of the seascape metrics has specific requirements of the sampling scale and quadrat density for robust estimation. Overall, the majority of the metrics were accurately identified by sampling scales equal to or coarser than 5 m × 5 m and quadrat densities equal to or larger than 30. The study indicates that special attention needs to be dedicated to the design of coral reef monitoring programmes, with decisions being based on the seascape metrics and statistics being determined. The results presented here are representative of the eastern South Africa coral reefs and are expected to be transferable to coral reefs with similar characteristics. The work presented here is limited to one study site and further research is required to confirm the findings.

**Keywords:** seascape metrics; structure-from-motion; FRAGSTATS; photogrammetry; sampling scale; quadrat density; sampling strategy; sampling framework

## 1. Introduction

Coral reefs provide key provisioning, cultural and regulating ecosystem services [1,2]. Their economic value has been estimated in recent studies through the ecosystem services theory developed by Samonte et al. [3], Seenprachawong [4] and the Millennium Ecosystem Assessment's classification [5]. Within the context of provisioning and cultural services, coral reefs provide an important protein source and a basin for livelihoods for fisheries in addition to scenic beauty for recreational tourism [6]. Regarding regulating services, coral reefs provide coastal protection by dissipating the waves energy [7] and contribute to the regulation of the coastal line erosion and sedimentation [6]. The benefits of coral reefs are therefore vast and varied. However, anthropogenic threats at the regional and global scale have considerably impacted coral reefs, with 19% of reefs considered completely lost and 60–75% of reefs threatened by 2011 [8–10]. The increase of extreme weather events impacting the coast [11] has also played a significant role in large-scale degradation. As a result, coral reef protection has become a priority in many governmental agendas (e.g., [12]). This has resulted in the development and implementation of scientific surveys and monitoring programs aimed at evaluating the causes, effects and extent of coral threats (e.g., sedimentation, bleaching and climate change) [13–15].

In general, wide-area (>1500 m<sup>2</sup>) coral reef monitoring methods are based on remote sensing approaches that range from autonomous or semi-autonomous underwater vehicles [13,16–19] to satellite and airborne imagery [20–23]. For the particular case of wide-area (>1500 m<sup>2</sup>) in situ monitoring, the key limitations are cost, access to the site and the spatio-temporal extent to be covered [15]. In situ refers hereinafter to all techniques that require human presence at the site to obtain relevant samples (e.g., photographs or biological samples), and its meaning is specific to this manuscript. In situ methodologies provide higher spatial resolution than wide-area (>1500 m<sup>2</sup>) remote sensing methods (e.g., satellites) and are essential for the understanding of very fine ecological processes [15,24]. New technologies and analytical solutions (e.g., autonomous and semi-autonomous underwater vehicles, boat-based systems and close range Structure-from-Motion (SfM)) have been developed and can help fulfil the need for wide-area (>1500 m<sup>2</sup>) high resolution data provision [13,18,19,25,26]. This scientific advance in coral reef monitoring relies on the integration of low cost off-the-shelf cameras and state of the art photogrammetric techniques (i.e., SfM) [27,28]. The resulting data products include high resolution (finer than 5 cm) Digital Elevation Models (DEMs), point clouds and two-dimensional mosaics [19,29,30], which enable the 2D and 3D analysis of coral reef ecological processes at different scales through the use of key metrics [19,25–27,31,32]. Examples of the use of these techniques include Burn [33], Chirayath [34], Gutierrez [35] and Lavy [36]. Burns [33] used 3D SfM-derived models to estimate key metrics that informed on changes to the benthic habitat along 25 m long transects and covering around 250 m<sup>2</sup>. Chirayath [34] applied SfM techniques to map a 15 km<sup>2</sup> coral reef area in the Shark Bay (Australia) and to generate an accurate bathymetric map from an unmanned aerial vehicle. Gutierrez [35] applied SfM to generate 3D models of the benthic organisms for taxonomic identification purposes, whereas Lavy [36] applied SfM techniques to derive morphological measurement of corals.

Several authors have looked at the application of seascape ecology metrics to characterize the ecological processes of coral reefs [37,38]. However, little effort has yet been made to define the appropriate sampling strategy to accurately determine each of the metrics; the ecological rationale for scale selection is usually unsupported [37]. Generally, scale selection is based on arbitrary choices or convention, albeit scale having an impact on seascape metric estimation [39]. The importance of standardized sampling protocols has already been recognized by several authors [37]. For example, Lecours et al. [24] recognizes the need for multiple scale approaches in benthic habitat mapping and states that sampling should be planned in order to describe those variables relevant for the study. Boström et al. [37] recognizes the design of a survey as a key future research priority for seascape ecology; the wide range of spatio-temporal scales used in seascape studies inhibits the ability to directly compare studies' outcomes, identify general patterns, predict consequences across systems and design coastal reserves based on relevant information. Kendall and Miller [39] underline the negative effects of changes in map resolution when representing ecological landscape indexes. Garrabou et al. [40,41]

proposed the calculation of landscape metrics at centimeter resolution in accord with the principles of landscape ecology [42].

There are multiple studies that [20,43–45] investigate the effect that the sampling design (i.e., the combined effect of scale, quadrat density and sampling strategy) has on metric estimation. For example, Costa et al. [20] carried out a comparative assessment for bathymetry and intensity characterization at two different spatial scales ( $4\text{ m} \times 5000\text{ m}$  and  $4\text{ m} \times 500\text{ m}$ ), whereas Pittman et al. [43] quantified seven different morphometrics at multiple scales (i.e., 15 m, 25 m, 50 m, 100 m, 200 m, 300 m radius) from a 4 m bathymetry grid. Both studies showed that the spatial scale had an influence on the derived metrics. Wedding et al. [44] used a stratified sampling strategy to estimate rugosity and compare it to rugosity estimates obtained from a DEM at four grid sizes (i.e., 4 cm, 10 cm, 15 cm and 25 cm). Results showed that the 4 m grid was the only grid size showing a significant positive association with the in situ rugosity. The author proposed the method as non-substitutive of the finer scale rugosity methods for characterizing coral reef communities, but as an effective alternative for broad scale assessments. Purkis et al. [45] used a kernel radius of 4 m, 8 m, 20 m and 40 m with an increment of 20 m–400 m to estimate rugosity and habitat. In their study, results indicated that the habitat of up to (but likely not exceeding) 40 m away, most strongly influenced the diversity and particularly the abundance of certain fish guilds.

Here, multiple sample scales and quadrat densities applied on a high resolution (1.8 cm) wide area ( $>1500\text{ m}^2$ ) dataset, where sample scale indicates the sampling quadrat size and quadrat density refers to the number of quadrats taken within a target area, will be compared. The aim of the study is to develop an SfM-based monitoring framework for the estimation of seascape metrics using semi-autonomous vehicles with embedded cameras for imagery collection for the case of the study area of Ponta do Ouro, Mozambique. This will be achieved through the following overarching objectives:

- (1) to quantify the trade-offs between sample scale and robustness in seascape metric estimation;
- (2) to quantify the trade-offs between sample quadrat density and robustness in seascape metrics estimation;
- (3) to define a set of guidelines for seascape metric estimation based on findings from (1) and (2).

## 2. Material and Methods

### 2.1. Study Site

The study area is located in the Partial Marine Reserve of Ponta do Ouro, Mozambique (Figure 1a) and is part of the Isimangaliso Wetland Park, which protects the southernmost tropical coral reefs of the African continent [46]. The coral reef system is dominated by non-accretive corals running parallel to the coastline at 1–2 km from the shore [47,48]. Outcrops are present (Figure 1b,c) and originate from fossilization of Late Pleistocene beaches and dunes [49] that form very flat structures [50]. The area is characterized by high levels of endemic species [51–53] with the coral cover being dominated by soft corals that are tolerant to strong wave energy and sediment resuspension [54–57].



**Figure 1.** (a) Location of the study site in the Partial Marine Protected Area of Ponta do Ouro (Mozambique); (b) detailed image showing the fossil dune outcrops along the sandy littoral; (c) detailed image showing the submerged outcrops at the dive site.

## 2.2. Data Acquisition

Data collection was carried out by two SCUBA divers using a Sierra Dive Xtras (Xtras, Ltd., Mukilteo, WA, USA) Diver Propulsion Vehicle (DPV) equipped with a GoPro Hero3 Silver (Woodman Labs, Inc., San Mateo, CA, USA) and an Asus Google Nexus 7 tablet (Google Inc., Mountain View, CA, USA) embedded within an Alltab dry case system (Alleco Ltd., Helsinki, Finland) (Figure 2). The camera was set to time-lapse mode, recording nadir images at 1 Hz frequency with a focal length equivalent to 21 mm. Inertial navigation data obtained from the gyroscope and the accelerometer were logged via an Ubica Underwater Position System (UUPS) [58] be-spoke application. The logged data were then used to derive camera pitch, yaw and roll.

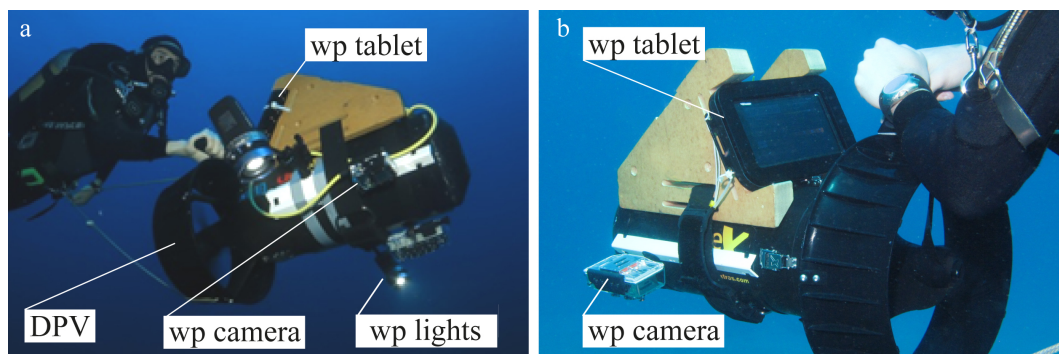


**Figure 2.** (a) A general photograph of the Diver Propulsion Vehicle (DPV) equipped with the Hero3 Silver camera, the waterproof tablet and the lights; (b) detailed image of the waterproof camera and tablet. “wp” stands for waterproof.

The sampling path was defined by two 50 m ancillary tapes distributed following homogeneous seascape characteristics identified in a pre-deployment survey (Figure 1c). The exact path followed by the diver was recorded via a towed buoy with an integrated Etrex10 GPS (Garmin Ltd., Lenexa, KS, USA). The GPS coordinates were recorded in Wide Area Augmentation System (WAAS) mode at 1 Hz frequency and projected into the Universal Transverse Mercator (UTM) fuse 36 Southern Hemisphere coordinate system, defined by the World Geodetic System (WGS84), within a Geographical Information System (GIS) environment (ArcGIS 10.1, Redlands, CA, USA). The diver maintained an average swimming speed of  $0.75 \text{ m s}^{-1}$  and an average distance to the sea bottom of 2.7 m, with the range being between 1.5 m and 3 m and with each frame covering  $3 \text{ m}^2$  (Figure 3a).

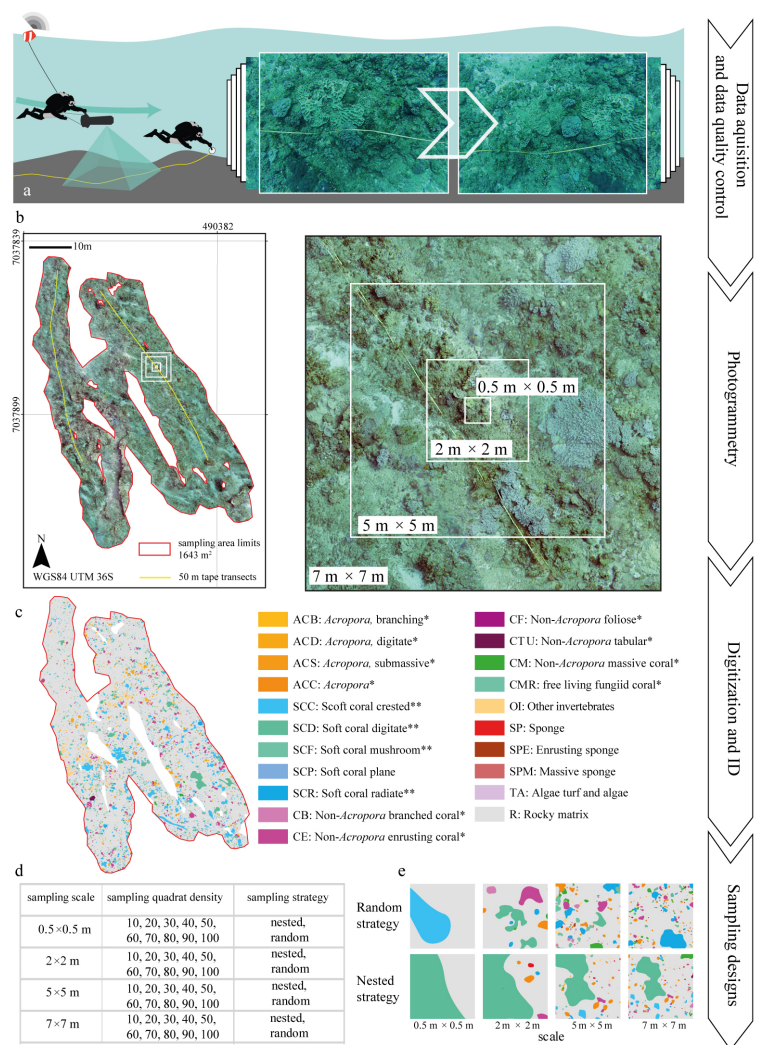


**Figure 3.** Schematic workflow overview for the field data collection and data analysis implemented: (a) transect deployment and image collection (left) and detailed example of the collected imagery (right); (b) processed orthoimage of the transects with the example of nested quadrats (left) and the detail of the nested sampling scales applied (right); (c) digitized output showing the abundance of different classes of benthic organisms; (d) summary of sampling scale, quadrat density and strategy applied; (e) graphical example of the digitized sessile organisms within different sampling scales. \* and \*\* refer to the classification proposed by Edinger and Risk [60] and the classes used by Schleyer and Celliers [49], respectively. ID stands for Identification Code.

Consecutive frames were taken with an approximate overlap of 70% along and 45% across the path. The sampling was performed in the central area of the reef covering a total of 1655 m<sup>2</sup> at an average depth of −22 m AMSL. All datasets were acquired on the 8 May 2015 during one single dive with a SCUBA dive. Data were collected during steady and calm sea-weather condition with good visibility (estimated 20 m) and avoiding the lowest and the highest tides.

All the underwater imagery was collected within 15 min. A total of four hours was required to set up the equipment on site (e.g., mount the camera, deploy the tape underwater, set up the parameters, implement the field briefing). An additional hour was required after the dive to check that all the imagery had been captured correctly and the UUPS had logged all of the required information. An extra 20 min were required to pack the equipment.

### 2.3. Photogrammetric Process and Digitization

A total of 1192 images collected were visually inspected, and only those with the right characteristics (i.e.,  $3200 \times 2400$  pixel high image quality and consecutive spatial coverage) were considered for further analysis (Figure 3a). A total of 8 h were required to visually inspect all the frames acquired. From the initial set of images, 1182 were included in the photogrammetry process. All the frames were captured at 1 cm resolution with a final orthoimage resolution of 1.8 cm. The metadata of each JPEG were stored in Exchangeable Image File format (EXIF) along with other camera parameters (e.g., camera model and optical lens characteristics) and directly loaded into Photoscan (Agisoft LLC., St. Petersburg, Russia). The exact position of each frame centroid was estimated by coupling the camera recording time with the GPS watch based on Roelfsema et al. [59]. pixGPS (BR Software, Asker, Norway) was used for that purpose. The coordinates for each of the frames were used to georeference (scale, translate and rotate) the imagery into the coordinate system defined by the World Geodetic System (WGS84) and to minimize geometric distortions. Image coregistration errors were automatically estimated by Photoscan as the difference between the positions measured through GPS and the coordinates derived from the imagery. The overall process to obtain the orthoimage took 12 h of processing time based on the performance of an Asus laptop (Beitou District, Taipei, Taiwan) with an Intel Core i7-3630QM 2.40-GHz processor (Intel Corporation, Santa Clara, CA, USA), 16 Gb RAM and graphic card NVIDIA GeForce GTX 670M (NVIDIA Corporation, Santa Clara, CA, USA).

Mega-epibenthic sessile organisms (i.e., seabed living organisms with a body diameter of 5 cm approximately) were manually identified and digitized to the finest possible taxonomic level and then clustered according with common morphological characteristics following the approach by Edinger and Risk [60] and the descriptions published by Schleyer and Celliers [49]. The morphological classification also accounted for non-coral organisms, such as sponges and other sessile invertebrates (i.e., tunicates and ascidians). The orthoimage was digitized manually and classified within ArcGIS (Figures 3b,c and 4a,b). The background rocky substrate, within which patches were embedded as “islands”, was considered as the seascape matrix (i.e., rocky matrix) following the island biogeography theory proposed by MacArthur and Wilson [61]. The digitization process required 21 days (i.e., 147 h at 7 h per day). A total of 7547 individual organisms were digitized from the orthoimage.

### 2.4. Seascape Metric Estimation

Seascape metrics were estimated from the orthoimage for a set of different sampling designs described by all the possible combinations of a range of sampling scales, quadrat densities and sampling strategies. Within the scope of this study, the sampling scale refers to the size of the sampling quadrats and ranged from  $0.5 \text{ m} \times 0.5 \text{ m}$ – $7 \text{ m} \times 7 \text{ m}$  (Figure 3d); the quadrat density is the number of quadrats taken within the target area and ranged from 10–100 in consecutive increments of 10 quadrats; and the sampling strategy refers to the spatial distribution of the samples (i.e., nested or random) (Figure 3e). The sampling designs were overlaid onto the orthoimage within ArcGIS.

Nested sampling approaches require the overlap of quadrat centroids of consecutively increasing scales. Each scale appears only once in each set of overlapped centroids, with each set being randomly distributed across the reef. The range of values considered for the sampling scale, quadrat density and sampling strategy was selected based on the size of the sessile organisms, their spatial distribution, the magnitude of the effects to be measured and standard sampling protocols for coral reefs [19,62–64]. A total of three replications were obtained for each combination of sample scale, quadrat density and sampling strategy to account for spatial variability. All quadrats were inspected to ensure that at least 60% of their surface fell within the extent of the coral reef area. Although the centroid of the quadrat was always forced to be within the surveyed area, this did not guarantee that all the quadrat fell within the boundary. Those quadrats with more than 40% of their surface falling outside the coral reef boundaries were excluded from the analysis. The spatial distribution of sampling quadrats was automated in ArcGIS using a range of tools (i.e., create random points, buffer, envelope feature

to polygon, iterate feature classes, clip, invert, merge and polygon to raster) within the ArcMAP model builder.

Seascape metrics were derived using FRAGSTATS v4 (Amherst, MA, USA) [65], a software developed to compute a wide variety of landscape metrics for categorical map patterns that has successfully been applied for seascape ecology [38–40,66]. Only metrics that could be automatically derived from FRAGSTATS were considered within this study because of their potential to enhance the autonomy of the framework. From the more traditional metrics used for coral reef characterization, only cover was calculated, as it is a key metric used to assess the benthic community composition.

FRAGSTATS estimates key landscape metrics, hereinafter referred to as seascape metrics, based on the disposition of the patches within the landscape (i.e., seascape). Here, a patch is each of the digitized individual polygons (Figure 4). A set of metrics defining area-density-edge, shape, contagion and interspersion, as well as diversity was selected based on their relevance to seascape ecology composition (Table 1).

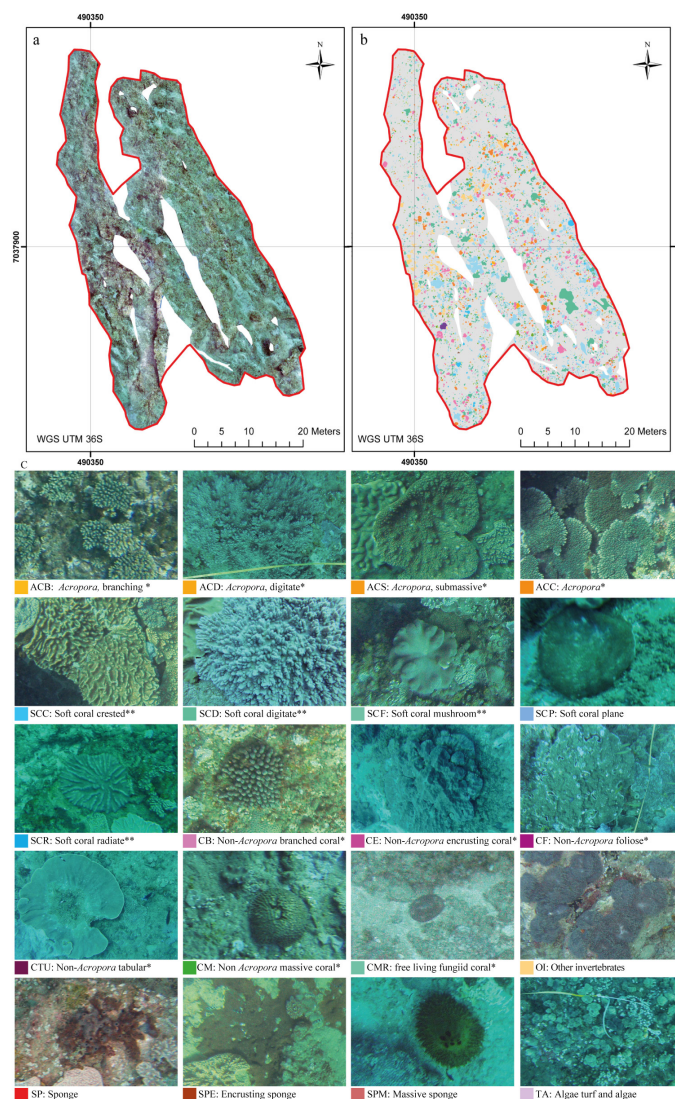


**Figure 4.** (a) The processed orthoimage; (b) the map of the digitized benthic organisms; (c) the configuration of the digitized sessile organism within the case study area of Ponta do Ouro Partial Marine Reserve (Mozambique). \* and \*\* refer to the classification proposed by Edinger and Risk [60] and the classes used by Schleyer and Celliers [49], respectively.

Area-density-edge metrics relate to the number and size of sessile organisms and the amount of edges created by them. Here, the edge is the border between adjacent patches. This group of metrics includes the Landscape Shape Index (LSI) and the Largest Patch Index (LPI) [65]. LSI informs about the morphological aggregation of the patches within a standardized seascape square. The value of LSI increases without limit from 1 upwards as the seascape becomes disaggregated, where 1 represents minimum disaggregation. LPI informs about the clumpiness of the seascape as the percentage value within a standardized seascape square. It is a measure of patch dominance; LPI values of 100% indicate that the seascape unit is dominated by a single patch. Both LSI and LPI provide information on the composition of the sessile organism communities in size per class and on the structure of the reef; seascapes that are highly subdivided into small patches are characteristics of low colonized substrates where colonies have difficulties settling and cannot reach typical dimensions. This can be caused by multiple factors, such as sediment resuspension and deposition or high wave energy [57].

Shape metrics (i.e., Perimeter Area Ratio (PARA) change) [65,67] are directly estimated from the shape of the organisms. In particular, PARA estimates the ratio between the perimeter and the area of all the patches within the seascape unit and provides information on the shape complexity of the patches in the seascape; an increase in the size of the patch results in a decrease in the value of PARA. PARA is always larger than 0 and does not have an upper limit. The PARA value could be interpreted as a good indicator of the growth conditions of corals; corals show constant radial allometric growth [68], but this can be affected by external factors, such as intra-specific and inter-specific competition and hydrodynamic conditions. Under affected allometric growth conditions, larger PARA values are to be expected.

Contagion and dispersion metrics (i.e., Aggregation Index (AI) and Division index (DIVISION)) [65] look at the seascape texture by examining the aggregation and intermix of the class of organisms. AI [65,69] quantifies the adjacencies per patch type within the seascape and informs on the homogeneity of the composition of the benthic communities. It ranges from 0% (maximum patch disaggregation) to 100% (maximum patch aggregation). High values of AI indicate that the classes of patches are more clustered within the landscape. This could inform about the reproductive biology of the species considered and the population dynamics; species with short larval dispersion tend to create clusters of individuals near the organism. These species are more sensitive to local extinctions [70]. Instead, DIVISION measures the heterogeneity of the seascape and estimates the variability in patch types within the seascape. DIVISION ranges from 0–1, where a 0 value indicates maximum aggregation, and values close to 1 indicate maximum disaggregation. These indexes provide information on the composition of the coral and the planar morphology of the colonies within the seascape; heterogeneous seascapes are composed by a varied benthic community or placed at the edge of the reef, where just a few individuals per specie are settled.

Diversity metrics focus on the number of organisms and their distribution within the seascape. They are an indication of the resilience of the coral reef and its ability to withstand significant disturbances [71]. Within this group, five key metrics have been estimated: Patch Richness (PR), Shannon's Diversity Index (SHDI), Simpson's Diversity Index (SIDI), Shannon's Evenness Index (SHEI) and Simpson's Evenness Index (SIEI) [65]. PR informs about the number of patches present within the seascape. SHDI [72] informs about the number of different patch types within the seascape and how evenly these types are distributed. SHDI can present any positive value from 0 upwards. Larger SHDI values represent greater evenness amongst patch types within the seascape. SIDI [73] informs about the probability that two entities (i.e., pixels) taken at random from the same seascape belong to different patch types and ranges between 0 and 1. Larger SIDI values indicate a greater probability that two pixels are from different patch types. Both SHEI and SIEI estimate the proportion of the maximum Shannon's or Simpson's diversity index, respectively. SHEI and SIEI range from 0–1, where 1 indicates that the area is distributed evenly among patch types.

**Table 1.** Seascape metrics estimated for the case study area of Ponta do Ouro Marine Reserve (Mozambique). The seascape metric descriptions are based on those for landscape analysis obtained from FRAGSTATS v4 [65]. All metrics are dimensionless except for the Largest Patch Index (LPI) (%), AI (%) and DIVISION (ratio). Here, patch refers to each of the digitized individual polygons falling within a given morphological class.

Metrics	Index	Description
Area Density Edge	Landscape Shape Index (LSI)	Normalized ratio of edge (i.e., patch perimeters) to area (i.e., seascape defined by the sampling scale) in which the total length of edge is compared to a seascape with a standard shape (square) of the same size and without any internal edge. LSI = 1 when the seascape consists of a single square patch; LSI increases without limit as the morphology becomes more disaggregated. LSI provides a simple measure of morphological aggregation or clumpiness.
	Largest Patch Index (LPI)	Percentage of the seascape comprised of the single largest patch. LPI approaches 0 when the largest patch is increasingly small. LPI = 100 when the entire seascape consists of a single patch; that is, when the largest patch comprises 100% of the seascape.
Shape	Perimeter Area Ratio (PARA)	Simple ratio of patch perimeter to area in which patch shape is confounded with patch size. The ratio is not standardized to a simple Euclidean shape (e.g., square); an increase in patch size will cause a decrease in the perimeter-area ratio.
Contagion Interspersion	Aggregation Index (AI)	The ratio of the observed number of like adjacencies to the maximum possible number of like adjacencies given the proportion of the seascape comprised of each patch type (%). The maximum number of like adjacencies is achieved when the morphological class is clumped into a single compact patch, which does not have to be a square.
	Division Index (DIVISION)	The probability that two randomly chosen pixels in the seascape are not situated in the same patch. Maximum values are achieved when the seascape is maximally subdivided; that is, when every pixel is a separate patch.
Diversity	Patch Richness (PR)	Number of patch types present in the seascape.
	Shannon's Diversity Index (SHDI)	Represent the amount of "information" per morphological class; larger values indicate a greater number of patch types and /or greater evenness among types.
	Simpson's Diversity Index (SIDI)	The probability that any two pixels selected at random would correspond to different patch types; the larger the values the greater the likelihood than any two randomly drawn pixels would be different patch types.
	Shannon's Evenness Index (SHEI)	Proportion of maximum Shannon's Diversity Index based on the distribution of area among patch types and typically given as the observed level diversity divided by the maximum possible diversity given the patch richness. SHEI = 1 when the area is distributed evenly among patch types.
	Simpson's Evenness Index (SIEI)	Proportion of maximum Simpson's Diversity Index based on the distribution of area among patch types and typically given as the observed level diversity divided by the maximum possible diversity given the patch richness. SIEI = 1 when the area is distributed evenly among patch types.

## 2.5. Data Analysis

Composition and abundance for the full extent of the mapped coral reef area were estimated based on the digitized sessile organism classes (Figures 3c and 4). The minimum and maximum cover of individual sessile organisms (total surface in m<sup>2</sup>) identified within each quadrat for each morphological class [49,60] were estimated. The average dimension, as well as the total count of individuals within each morphological class were also reported. Robustness in metric estimation was assessed for each sampling design based on the difference between the metric value estimated for a specific sampling design and (i) that obtained for the whole surveyed area or (ii) that obtained for the

most comprehensive sampling design considered (i.e., 7 m × 7 m and 100 quadrats). The effect on both measures of central tendency (e.g., mean, median) and dispersion (e.g., range, standard deviation) was assessed. Descriptive statistics and box-plots were used for that purpose. General trend patterns were derived from these observations and used to compile a set of general guidelines for coral reef sampling.

### 3. Results

The line transect defined by the metric tape accounted for 650 m. The coregistration error of the generated orthoimage was 4.08 m and 6.8 m for the  $x$  and  $y$  axis, respectively. Within the whole mapped area (1655 m<sup>2</sup>), the benthic organisms covered 335.54 m<sup>2</sup>, which equates to a total cover of 20.27%.

The coral reef was dominated by soft (Alcyonacea, 62.1% of the total cover) and hard corals (Scleractinia, 31.00% of the total cover) (Figure 5). Within the soft corals, the dominant morphological classes were (i) Soft Crested Coral (SCC) (soft corals that are rigid with mounted parallel lobes and low in profile) and (ii) Soft Corals with Digitate lobules (SCD). These groups presented the largest individual organism cover values (7 m<sup>2</sup>) and were represented by the genera *Lobophytum*, *Sinularia* and *Sarcophyton* (Table 2). Hard corals were mainly represented by the genus *Acropora* (44.32% of the total hard colony community). The more frequent class in the group was *Acropora* with digitated and stubby branches (ACD), presenting also the largest surface dimensions (Table 2).

Non-*Acropora* Massive or Multilobate Corals (CM) include *Platygyra* spp., *Montastrea* spp., *Galaxea* spp., *Favites* spp., *Favia* spp. and *Turbinaria* sp.. The average size for this morphological class was 0.019 m<sup>2</sup>. In addition to the above groups, 141 colonies of free-living fungiid corals were identified. These showed an average dimension of 0.006129 m<sup>2</sup> (Table 2) and also included 11 encrusting and dome-shaped sponges. The Other Invertebrates (OI) presented the largest variance in surface dimension with the tunicate *Atrioalum robustum*, accounting for 0.0008 m<sup>2</sup>, and the actinias *Stichodactyla* spp., accounting for 1.04 m<sup>2</sup>. The background rocky substrate accounted for 1150.55 m<sup>2</sup> of the total area (69.52%). The 10.27% (168.84 m<sup>2</sup>) of the overall coral reef area sampled, where individual organisms could not be identified, was not digitized.

The exclusion of quadrats with more than 40% of the area falling outside the coral reef boundary or presenting non-textured classes did not influence the overall analysis; the number of samples available was large enough for the robust estimation of the descriptive statistics, boxplots and associated metrics of species abundance and composition (Table 3).

The effect of scale, quadrant density and sampling strategy on cover estimation is summarized in Figure 5. Sampling scales coarser than 5 m × 5 m provide similar cover estimates to those obtained for the overall surveyed area, with the finest scale (0.5 m × 0.5 m) failing to accurately represent cover estimates. This pattern is more noticeable for random sampling strategies than for nested strategies. Regarding the quadrat density applied, no particular patterns can be observed as the number of quadrats used in the survey is increased. However, sampling designs where the combined area surveyed by the quadrats contains in excess of 100 m<sup>2</sup> of benthic organisms closely resembles the cover distributions observed within the whole surveyed area.

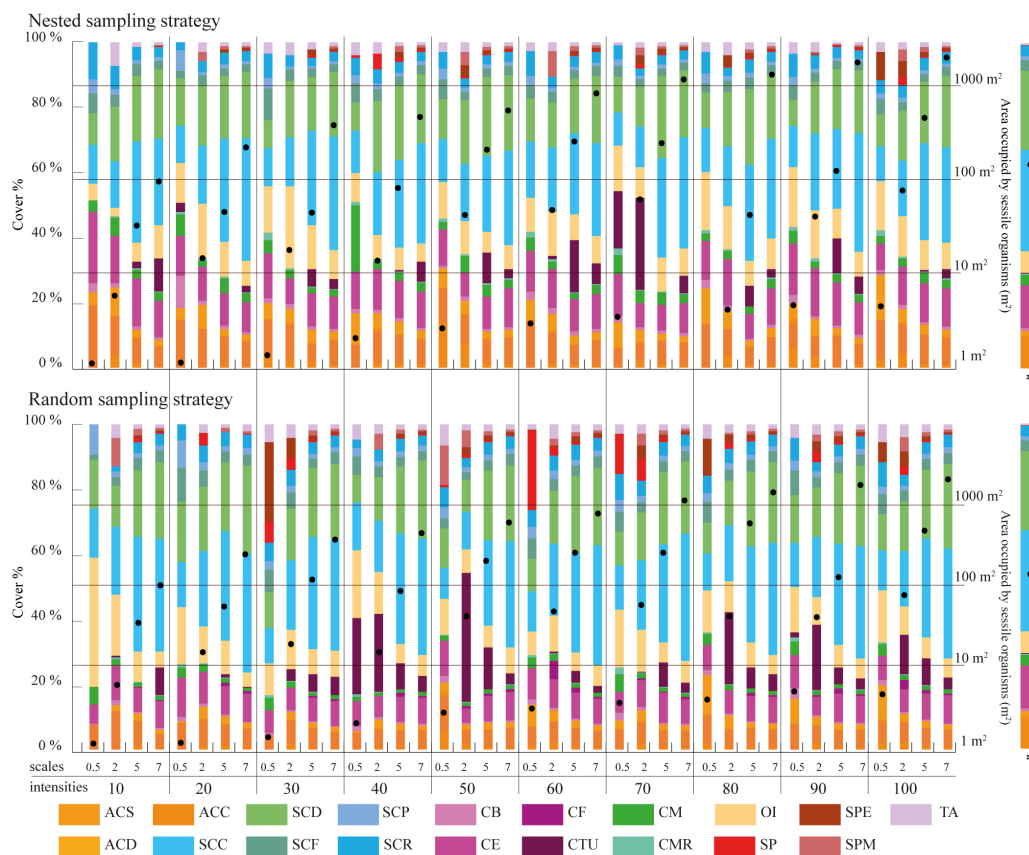


**Figure 5.** Percentage of cover per morphological class for each sampling design considered in the study. The proportion is estimated as the ratio between the area occupied by each morphological class over the total area covered by the sessile organisms within each sampling design. The values presented refer to the average cover of the three replicates taken within each sampling design. The “\*” indicates the total area covered by the sessile organisms in each sampling design estimated as the average of the three replicates taken. The last column shows the cover per morphological class for the totality of the coral reef surveyed.

For area-density-edge metrics, the overall area surveyed scores an LSI value of 2.91 (Table 4). The LPI value for the sampled coral reef is 0.47% (Table 4). The LSI values for independent quadrats range between one and eight, showing that there is spatial heterogeneity in aggregation across the coral reef. The dispersion of LPI values obtained within some of the sampling design tested is large, with LPI values ranging from 0%–100% in some cases. For both LSI and LPI, the sampling quadrat density has a larger impact on the estimation of the measures of dispersion (e.g., range, standard deviation) than on the estimation of measures of central tendency (e.g., mean, median). For LSI, quadrat densities above 70 are required to characterize the measures of dispersion for nested strategies to the same level as the most comprehensive quadrat density applied (i.e., 100), whereas quadrat densities above 40 are required for random strategies. For LPI, quadrat densities above 40 and 30 are required to characterize the measures of dispersion for nested and random strategies, respectively. In contrast, the sampling scale has a larger impact on the measures of central tendency than on the measures of dispersion. The finest scale (0.5 m × 0.5 m) presents the largest deviations from the seascape metrics obtained for the overall coral reef area. For LPI, sampling scales of 5 m × 5 m and 7 m × 7 m provided good approximations to the metrics obtained for the totality of the coral reef area for both nested and random strategies (Figures 6 and 7). However, for LSI, coarse scales (7 m × 7 m) were required for both nested and random strategies.

**Table 2.** Description of the key morphological classes of benthic organisms and their count, maximum (max), minimum (min) and average dimensions (m<sup>2</sup>), identified within the coral reef studied in the Partial Marine Reserve of Ponta do Ouro (Mozambique).

Acronym	Description	Count	Average Dimension	Max Dimension	Min Dimension
ACB	<i>Acropora</i> , branching (e.g., <i>A. austera</i> )	15	0.384 ± 0.016	0.716	0.225
ACD	<i>Acropora</i> , digitate, stubby (e.g., <i>A. humilis</i> )	465	0.069 ± 0.010	0.821	0.044
ACS	<i>Acropora</i> , columns and blades, very stout (e.g., <i>A. palifera</i> and <i>A. cuneata</i> )	109	0.054 ± 0.068	0.467	0.001
ACC	<i>Acropora</i> , stout branches, low bushy shape	20	0.045 ± 0.041	0.148	0.005
CM	Non- <i>Acropora</i> massive or multilobate corals (e.g., <i>Platygyra</i> spp. and <i>Galaxea</i> spp.)	559	0.019 ± 0.038	0.544	0.0005
CE	Low relief, often small colonies (e.g. <i>Porites</i> spp.)	533	0.083 ± 0.112	1.281	0.002
CTU	Tabular coral (e.g., <i>Turbinaria</i> sp.)	4	0.300 ± 0.573	1.160	0.009
CMR	Free-living fungiid corals	141	0.006 ± 0.004	0.034	0.015
CB	Branching non- <i>Acropora</i> corals (e.g., <i>Pocillopora</i> spp.)	275	0.011 ± 0.012	0.089	0.065
CF	Foliose, either horizontal or vertical, non- <i>Acropora</i> , (e.g., <i>Montipora</i> spp., <i>Echinopora</i> spp.)	2	0.065 ± 0.069	0.1138	0.0164
OI	Other invertebrates inclusive of gasterops, tunicates, echinoderms and other hexacorals	339	0.067 ± 0.134	1.044	0.00008
SCF	Erect in profile, but soft and pliable with an expanded disk and stalk (e.g., <i>Sarcophyton</i> spp.)	461	0.023 ± 0.021	0.137	0.046
SCD	Soft and pliable colonies (e.g., <i>Sinularia</i> spp.)	1916	0.042 ± 0.205	7.6134	0.045
SCC	Low in profile and rigid with mounded radial (e.g., <i>L. latilobatum</i> )	1721	0.061 ± 0.197	4.376	0.645
SCR	Low in profile and rigid with erect radial or parallel lobes (e.g., <i>L. crassum</i> ).	342	0.032 ± 0.068	0.974	0.002
SCP	Low in profile and plane on the surface (e.g., <i>L. depressum</i> )	466	0.009 ± 0.007	0.0562	0.0007
SP	General sponges	6	0.041 ± 0.031	0.092	0.001
SPM	Massive or dome-like sponges	3	0.075 ± 0.038	0.119	0.046
SPE	Encrusting sponges	2	0.070 ± 0.022	0.086	0.055
TA	Algae and algal turf	168	0.010 ± 0.018	0.144	0.0004

The PARA shape metric (Figures 6 and 7) reaches values of  $4.5 \times 10^5$  (Table 4) for the whole area surveyed. The multiple sampling scales considered report different results in terms of measures of dispersion. Scales finer than  $2 \text{ m} \times 2 \text{ m}$  report dispersion values considerably larger than coarser scales and are characterized by PARA metric overestimation. The pattern is more prominent for nested strategies, where PARA values of individual quadrats reach magnitudes of  $3 \times 10^6$ , whereas for random strategies, the maximum values do not exceed magnitudes of  $1.6 \times 10^6$ . The quadrat density also influences the estimation of the measures of dispersion, with the range of PARA decreasing as the number of quadrats increases for both nested and random sampling strategies. Quadrat densities of 40 and 30 provide similar results to those obtained for the maximum quadrat densities applied (i.e., 100) for nested and random strategies, respectively.

**Table 3.** Sample size per combination of sampling scale, quadrat density and strategy considered, after exclusion of non-valid samples (i.e., quadrats with more than 40% of the area falling outside the coral reef boundary or presenting non-textured morphological class).

Scale	0.5 m × 0.5 m		2 m × 2 m		5 m × 5 m		7 m × 7 m		Expected
Density	Random	Nested	Random	Nested	Random	Nested	Random	Nested	
10	24	25	29	28	28	28	27	27	30
20	50	49	54	56	53	53	44	44	60
30	73	70	78	83	80	80	73	73	90
40	91	98	113	116	108	108	109	109	120
50	127	117	142	142	136	136	130	130	150
60	145	146	178	176	167	167	161	162	180
70	164	161	201	204	202	202	190	190	210
80	191	187	237	234	225	225	223	223	240
90	213	216	260	265	244	245	250	250	270
100	240	239	287	290	291	290	270	282	300

**Table 4.** Seascape metric values obtained for the total coral reef area surveyed. The metrics reported include: Landscape Shape Index (LSI), Large Patch Index (LPI), Perimeter Area Ratio (PARA), Aggregation Index (AI), Division Index (DIVISION), Patch Richness (PR), Shannon's Diversity Index (SHDI), Simpson's Diversity Index (SIDI), Shannon's Evenness Index (SHEI) and Simpson's Evenness Index (SIEI).

Acronym	Value	Acronym	Value
LSI	2.91	LPI	0.47%
PARA	4.52 e <sup>5</sup>	AI	95.61%
DIVISION	0.99%	PR	23
SHDI	1.94	SIDI	0.78
SHEI	0.62	SIEI	0.83

The contagion and dispersion metric AI scores 95.6% (Table 4) for the case study area. The value of AI for independent quadrats oscillates between 70% and 100% approximately. For nested strategies, scales equal to or coarser than 5 m × 5 m underestimate the value of AI, whereas scales equal to or finer than 2 m × 2 m overestimate the value of the index. A similar pattern is observed for random strategies where scales equal to or coarser than 2 m × 2 m underestimate the metric value, and scales of 0.5 m × 0.5 m overestimate it. For both nested and random strategies, the finest scale considered (0.5 m × 0.5 m) results in large dispersion measurements, whereas coarser scales (i.e., coarser than 2 m × 2 m and 5 m × 5 m for nested and random, respectively) present similar dispersion estimates amongst each other. Quadrat density also influences the estimation of the measures of dispersion, with quadrat densities above 20 and 30 providing similar dispersion estimates to more dense designs for nested and random strategies, respectively.

In the particular case of DIVISION, the value for the overall area is 0.99% (Table 4). The DIVISION values of independent quadrats range from its plausible minimum to its maximum, this indicating that the index is highly dependent on the spatial heterogeneity of the site. The effect of sampling design for both nested and random strategies follows a similar pattern; measures of central tendency become more accurate as the quadrat scale increases, with scales finer than 2 m × 2 m reporting slight departures from the metric value obtained for the overall coral reef area. Sampling quadrat densities equal to or larger than 40 provide estimations of the dispersion measures close to those obtained for the most comprehensive density considered (i.e., 100).

The diversity metrics PR (23), SHDI (1.94), SIDI (0.78), SHEI (0.62) and SIEI (0.83) obtained for the overall area are also affected by changes in sampling design (Table 4, Figures 8 and 9). For PR, none of the sampling designs considered in this study capture the total number of different patch types present within the seascape for both nested and random sampling strategies. The mean PR obtained for independent sampling designs does not exceed a value of 14 in any instance, with PR

values obtained for individual quadrats ranging from 0–18. Sampling scale has an important effect on the estimation of measures of central tendency and dispersion for PR; the larger the scale, the larger the number of different patch types identified. The fine scales tested (equal or finer than  $2\text{ m} \times 2\text{ m}$ ) do not provide representative values of PR. The effect of quadrat density is not so apparent, with quadrat densities of 10 providing similar results in terms of measures of dispersion and central tendency to those obtained with 100 quadrats.

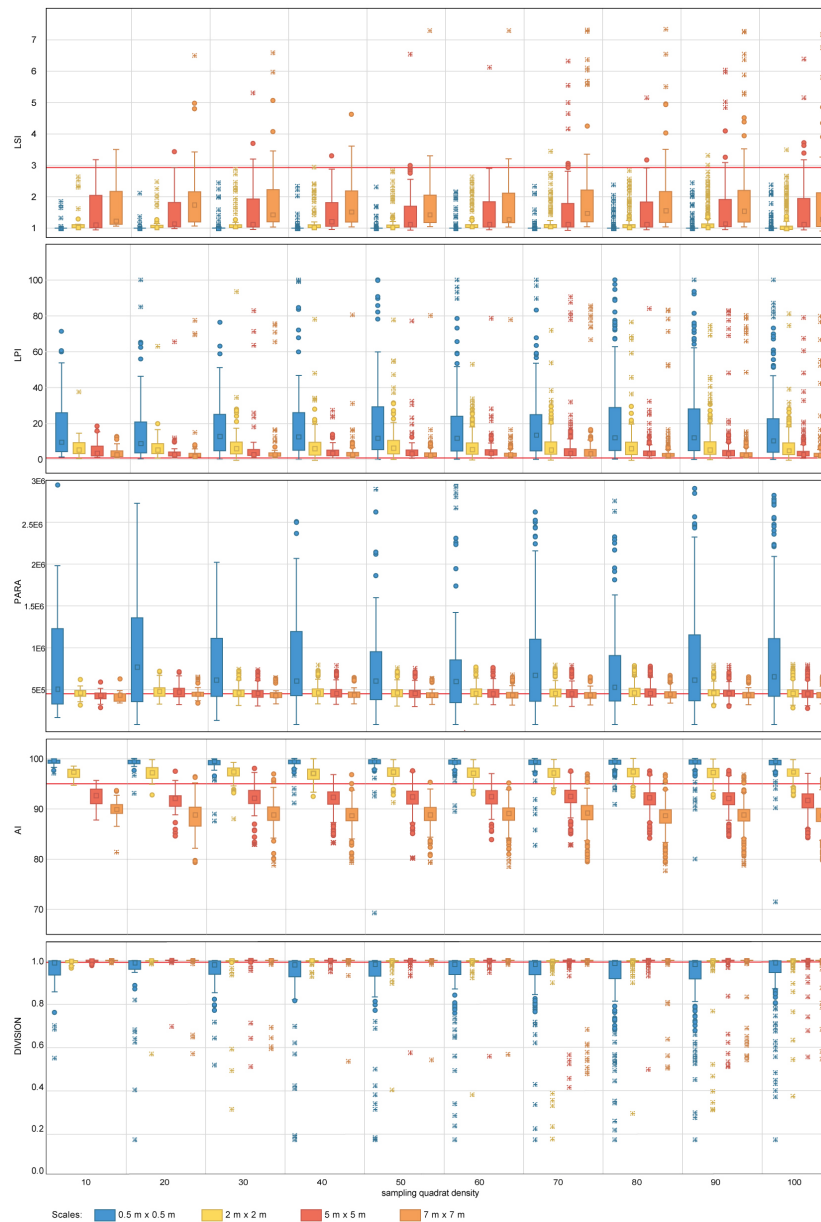


**Figure 6.** Area-density-edge, shape, contagion and interspersion metric values obtained for the nested sampling strategy for the range of scales and quadrat densities considered. The red horizontal line indicates the metric value obtained on the total area mapped. LSI, LPI, PARA, AI and DIVISION stand for Landscape Shape Index, Largest Patch Index, Perimeter Area Ration Mean, Aggregation Index and Division Index, respectively. The boxplots show the first, second (median), third and fourth quartiles. Circles and crosses indicate outliers and extreme values, respectively.

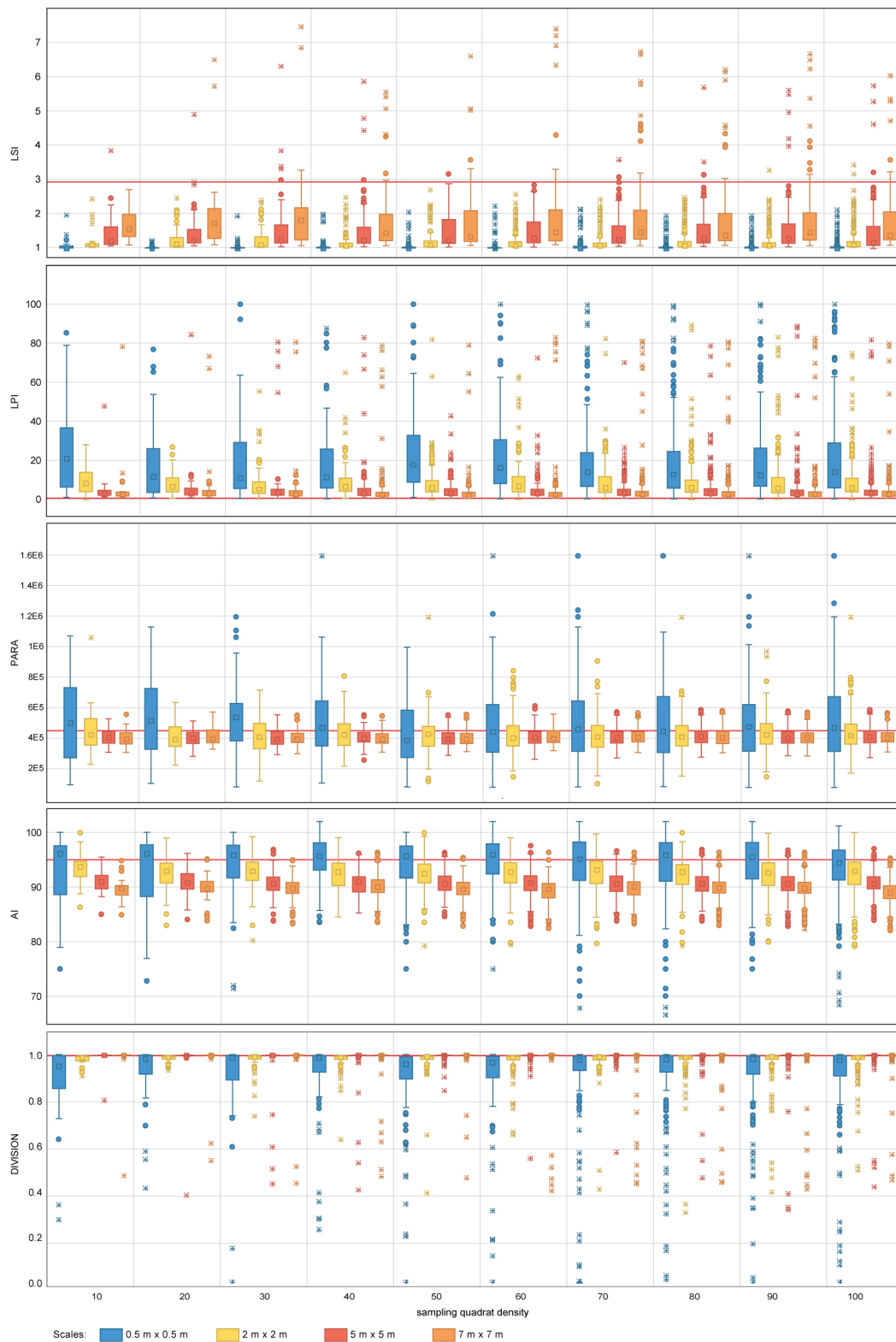


**Figure 7.** Area-density-edge, shape, contagion and interspersion metric values obtained for the random sampling strategy for the range of scales and quadrat densities considered. The red horizontal line indicates the metric value obtained on the total area mapped. LSI, LPI, PARA, AI and DIVISION stand for Landscape Shape Index, Largest Patch Index, Perimeter Area Ration Mean, Aggregation Index and Division Index, respectively. The boxplots show the first, second (median), third and fourth quartiles. Circles and crosses indicate outliers and extreme values, respectively.

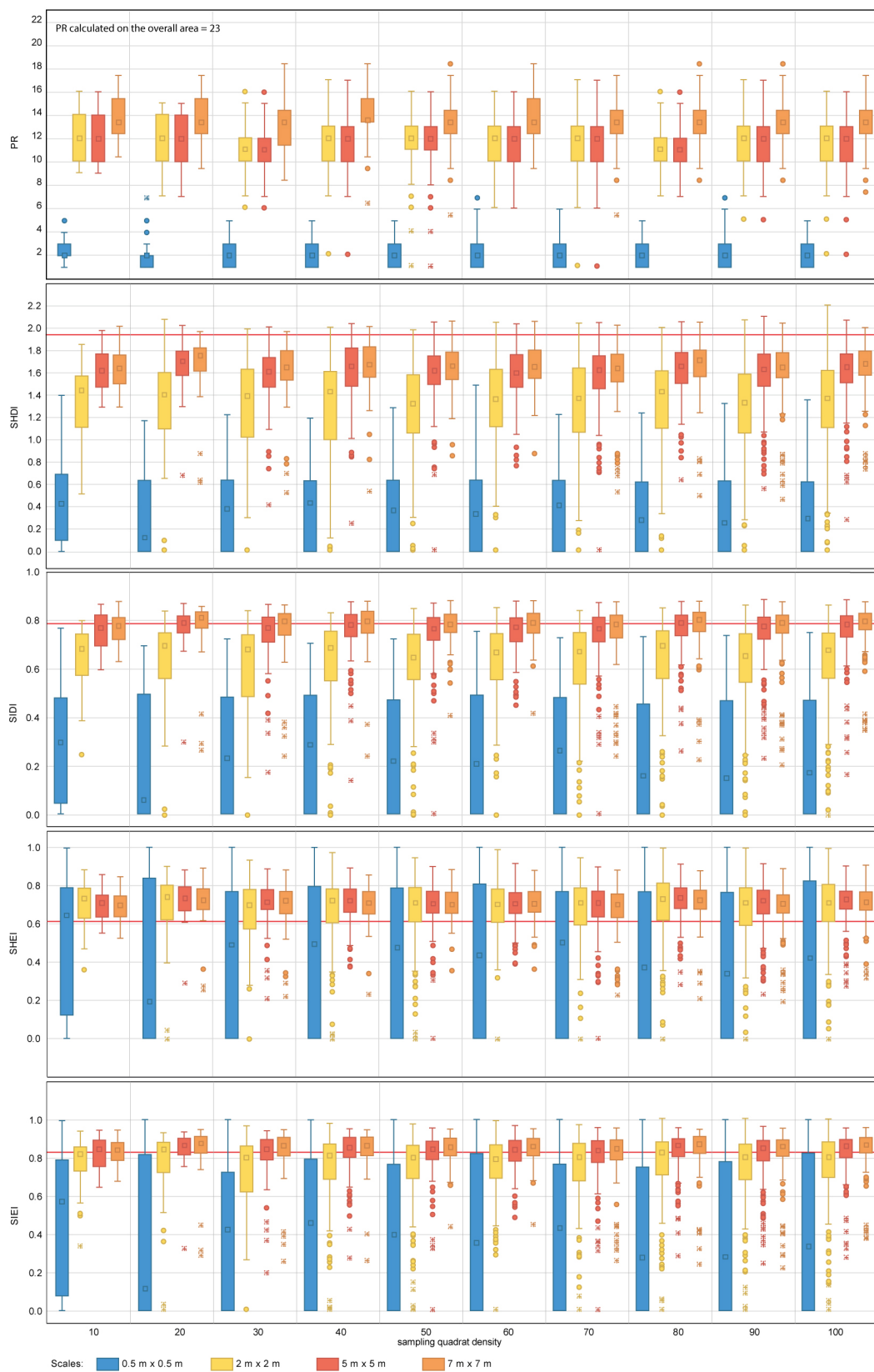


**Figure 8.** Diversity metric values obtained for the nested sampling strategy for the range of scales and quadrat densities considered. The red horizontal line indicates the metric value obtained for the total area mapped. PR, SHDI, SIDI, SHEI and SIEI stand for Patch Richness, Shannon’s Diversity Index, Simpson’s Diversity index, Shannon’s Evenness Index and Simpson’s Evenness Index, respectively. The boxplots show the first, second (median), third and fourth quartiles. Circles and crosses indicate outliers and extreme values, respectively.

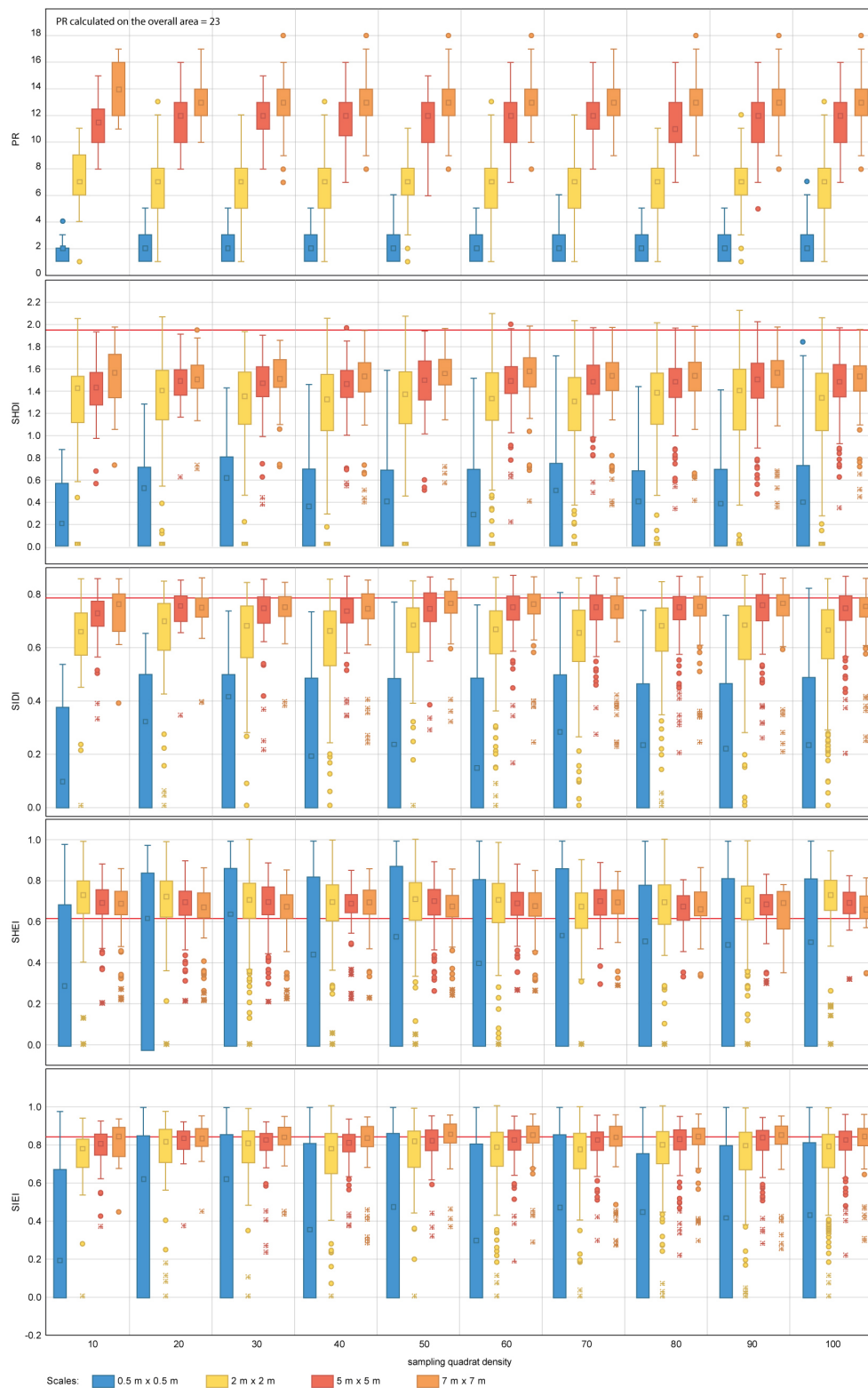


**Figure 9.** Diversity metric values obtained for the random sampling strategy for the range of scales and quadrat densities considered. The red horizontal line indicates the metric value obtained for the total area mapped. PR, SHDI, SIDI, SHEI and SIEI stand for Patch Richness, Shannon’s Diversity Index, Simpson’s Diversity index, Shannon’s Evenness Index and Simpson’s Evenness Index, respectively. The boxplots show the first, second (median), third and fourth quartiles. Circles and crosses indicate outliers and extreme values, respectively.

For SHDI and SIDI, the sampling design has a considerable effect on the estimation of the values of dispersion and central tendency, for both nested and random designs. Sampling scales equal to or finer than  $5\text{ m} \times 5\text{ m}$  for SHDI and  $2\text{ m} \times 2\text{ m}$  for SIDI fail to provide reliable metric estimates. The values of SHDI for individual quadrats oscillate between zero and two, with SIDI oscillating between zero and 0.9. SHEI and SIEI present a similar pattern to that described for SHDI and SIDI. However, for both metrics, sampling scales equal to or finer than  $2\text{ m} \times 2\text{ m}$  fail to provide close estimates of central tendency.

#### 4. Discussion

The results herein presented inform about the effect that sampling scale, quadrat density and strategy have on the estimation of specific seascape metrics and address the following objectives: (1) to quantify the trade-offs between sample scale and robustness in seascape metric estimation; (2) to quantify the trade-offs between sample quadrat density and robustness in seascape metric estimation; and (3) to develop a set of guidelines for seascape metric estimation based on the findings from (1) and (2). We acknowledge that other authors [40,66,74,75] successfully estimated those seascape metrics, and their experience has been fundamental for the selection of parameters in this study. For example, Hawkins and Hartnoll [74] estimated the species richness in intertidal benthic communities and highlighted the importance of calibrating the sample area based on the organism dimensions. They showed the effect that sample area had on different communities with different abundance and richness in species. Teixido [66] estimated a set of FRAGSTAT metrics for the characterization of the Antarctic mega-benthic communities across six stations. In their study, only one picture with a  $1\text{ m}^2$  footprint was taken at each station. The results indicated that the set of metrics used to characterize a coral reef must be defined and tailored to the case study area. Sleeman et al. [75] tested several metrics on seagrass meadow and reported the importance of defining a standard area for a meaningful interpretation of the ecological relevance of the metric. Garrabou et al. [40] investigated the spatial and temporal dynamics on rocky bottom benthic communities and successfully introduced the novel use of a set of area-perimeter-edge, shape, contagion interspersion and diversity metrics. However, none of these studies have assessed the combined effect of sampling scale, quadrat density and sampling strategy for the estimation of seascape metrics for high resolution coral reef sampling and SfM analysis.

Within the scope of Objectives (1) and (2), the area-density-edge seascape metrics obtained for the case study area of Ponta Do Ouro describe a coral reef that is disaggregated (LSI values around three) with low morphological class dominance (LPI = 0.47%). This is consistent with the cover value registered (69.52%), which indicates that the patches are dispersed within the rocky matrix. The LSI and LPI metrics also indicate that the sessile organisms within the surveyed area are present in a variety of dimensions. Based on the work by Schleyer [57], this could be the result of abrasion, caused by the combined effect of re-suspended sediments and waves energy, affecting the growth of both soft and hard corals. As a reference, in [66], the Antarctic benthic communities analyzed scored LSI values between 2.88 and 7.47. These communities are characterized by multistoreyed assemblages, intermediate to high species richness [76] and patchy distributions [77].

The description for the case study area of Ponta do Ouro may change depending on the sampling design implemented. For the area-density-edge metrics, quadrat densities below 70 for nested approaches and 40 for random would have failed to capture the spatial heterogeneity of LSI within the landscape (Table 5). For LPI, a similar pattern is encountered for quadrat densities below 40 and 30 for nested and random strategies, respectively. As a result, the seascape would have been assumed to have a homogeneous distribution of colonies, aggregation, clumpiness and dominance values based on the configuration described by the few quadrats sampled. Similarly, the finest sampling scales tested would have failed to provide representative values of area-density-edge metrics for the coral reef area. The metrics would have indicated that the reef is slightly more aggregated than observed and dominated by specific morphological classes. This would have had considerable implications in the assessment of the conservation status of the coral reef, its communities and their roles in supporting

ecosystem services. For example, an increase in habitat structural complexity generated by the presence of *Acropora austera* (ACB) has already been identified to support the diversity and abundance of the fish assemblages on South African coral reefs [78]. If representative metrics of both dispersion and central tendency are to be estimated to characterize area-density-edge metrics (i.e., LSI, LPI) for the case study area, the recommended quadrat densities provided in Table 5 are to be applied.

**Table 5.** Suggested sampling designs for the seascape metrics considered in this study for the case study area of Ponta do Ouro (Mozambique). The metrics reported include: Landscape Shape Index (LSI), Large Patch Index (LPI), Perimeter Area Ratio (PARA), Aggregation Index (AI), Division Index (DIVISION), Patch Richness (PR), Shannon’s Diversity Index (SHDI), Simpson’s Diversity Index (SIDI), Shannon’s Evenness Index (SHEI) and Simpson’s Evenness Index (SIEI).

Metric	Random		Nested	
	Scale	Quadrat Density	Scale	Quadrat Density
LSI	7 × 7	40	7 × 7	70
LPI	5 × 5	30	5 × 5	40
PARA	5 × 5	30	2 × 2	40
AI	5 × 5	20	2 × 2	30
DIVISION	2 × 2	40	2 × 2	40
PR	7 × 7	10	7 × 7	10
SHDI	7 × 7	10	7 × 7	10
SIDI	5 × 5	10	5 × 5	10
SHEI	5 × 5	10	5 × 5	10
SIEI	5 × 5	10	5 × 5	10

The PARA shape metric obtained for the overall surveyed area and field observations indicates that the expected radial allometric growth of the colonies has not been disturbed and that the growth conditions within the area are suitable for all the coral colonies to settle, develop and reach typical dimensions. However, the estimation of metrics of dispersion is highly affected by the sampling scale, quadrat density and strategy selected with the maximum PARA between  $1.6 \times 10^6$  and  $3 \times 10^6$  depending on the sampling design implemented. It is difficult to argue whether this level is meaningful from an ecological perspective, as no typology exists on the expected PARA value for coral reefs. However, based on in-field observations and the results for the most comprehensive sampling design applied (7 m × 7 m and 100 quadrats), information on how PARA relates to the spatial variability of coral growth can be derived. Results are more likely to indicate that the coral reef is dominated by smaller organisms than those present when using sampling scales finer than 2 m × 2 m. This could drive the assessment of the coral reef towards a more degraded status than it is. In addition, scales finer than 2 m × 2 m provide highly variable PARA measurements between independent quadrats and, therefore, overestimate the spatial heterogeneity of PARA within the area of interest. This is probably related to the dimensions of the organisms encountered (Table 2); many of the morphological classes identified are larger than the sampling area covered by any of the 0.5 m × 0.5 m (total area of 0.025 m<sup>2</sup>) and the 2 m × 2 m change<sup>2</sup> quadrats (total area of 4 m<sup>2</sup>). This sampling scale fails to capture the individual organisms in full and provide a biased estimation of PARA. In addition, fine sampling scales underestimate the perimeter of the organisms. This is because the perimeter of those organisms that are not included in full within the quadrat is not accounted for. The selection of quadrat density also plays a key role in the robust estimation of the spatial heterogeneity of PARA within the area of interest. For that purpose, quadrat densities below 30 and 40 are required for nested and random strategies, respectively. The use of lower quadrat densities may result in assessments that portray the growth of colonies within the surveyed area to be more heterogeneous (i.e., degraded) than it actually is (Table 5).

For the contagion and dispersion seascape metrics (AI and DIVISION), the overall metrics for the area indicate that most organisms colonizing the coral reef present relatively small dimensions,

are dispersed across the rocky matrix and are characterized by homogeneous distributions across the area. Results show that the sampling design has an influence on the estimation of AI with different combinations of scales and quadrat densities resulting in over and underestimations of AI measures of dispersion and central tendency. AI underestimation will portray the coral reef to be more aggregated than it is, whereas overestimations will result in a more positive assessment of the overall impact within the area. He [69] demonstrated that AI is strongly dependent (non-linear relationship) on the number of patches present within the landscape, and the identification for a sampling design that optimizes AI estimation is therefore difficult. For the case study area of Ponta do Ouro, sampling designs of  $20 \times (7 \text{ m} \times 7 \text{ m})$  and  $30 \times (5 \text{ m} \times 5 \text{ m})$  quadrats, for nested and random strategies respectively, provided good approximations to the values observed for the whole surveyed area. Fine sampling scales (equal to or finer than  $2 \text{ m} \times 2 \text{ m}$  for nested and  $0.5 \text{ m} \times 0.5 \text{ m}$  for random strategies) did not provide as good estimates as coarser scales; AI and its spatial heterogeneity were systematically overestimated. This is probably due to the dimensions of the individual organisms as described for the PARA metric. If these fine scales are applied, the systematic overestimation of AI and its spatial heterogeneity will result in biased coral reef assessment. For DIVISION, fine sampling scales (finer than  $2 \text{ m} \times 2 \text{ m}$ ) and reduced quadrat densities ( $<40$ ) translate into underestimation of the measures of central tendency and dispersion. In brief, these sampling designs will portray the coral reef to be more aggregated and less spatially heterogeneous than it is.

The group of diversity metrics (PR, SHDI, SIDI, SHEI and SIEI) presents a common pattern of response to changes in sampling design. Overall, the metrics indicate that the coral reef is diverse, and its area is proportionally distributed in accordance with their presence within the seascape. For the specific case of PR, scales finer than  $2 \text{ m} \times 2 \text{ m}$  fail to provide a representative value of PR. As per previous metrics, this may be explained by the size configuration of organisms within the seascape. None of the scales tested reached the PR value obtained for the overall coral reef area (i.e., 23). It is therefore difficult to suggest an optimal sampling scale for the case study area and impractical to make suggestions for other coral reefs. However, from the results obtained, scales of  $7 \text{ m} \times 7 \text{ m}$  are the best suited from those tested for the estimation of PR. In addition, the variability of PR values between individual quadrats indicates that this metric is also highly sensitive to the presence of spatial heterogeneity within the seascape. Spatial heterogeneity can be captured through the inclusion of further quadrats within the sampling design. For the case study area of Ponta do Ouro, quadrat densities as low as 10 provided similar estimates of PR measures of dispersion and central tendency as the most comprehensive densities applied (i.e., 100). Finer scales and densities than those suggested here (Table 5) will result in the coral reef being portrayed as less diverse and more heterogeneous than it really is.

For the SHDI and SIDI metrics, the sampling scale is key to reliable metric characterization. For SHDI, scales equal to or finer than  $2 \text{ m} \times 2 \text{ m}$  would have been more likely to portray the coral reef as less diverse (i.e., more degraded) and, therefore, less suited to host multiple colonies than it is. Similar results would have been obtained if scales equal to or finer than  $5 \text{ m} \times 5 \text{ m}$  would have been used for SIDI. The outcomes would have indicated that the reef is dominated by specific species that are more suited to colonize the available space. For both indexes, the variation in independent quadrat values indicates that the metrics are highly susceptible to the spatial heterogeneity. In the case of SHDI, it is difficult to assess whether the variation is significant from an ecological point of view, as the index is not capped in the upper limit. The SIDI index can adopt values comprised between zero and one, where zero indicates null diversity and one maximum diversity. In the case of the studied area, where the values of SIDI for individual quadrats oscillate between zero and 0.9, it is essential to ensure that the spatial heterogeneity within the site is captured with the sampling design implemented. The same rationale applies to SHEI and SIEI, which are derived calculations from SHDI and SIDI. For both SHEI and SIEI, the recommended sampling scales should be equal to or coarser than  $5 \text{ m} \times 5 \text{ m}$ . This is consistent with the results shown in [79], where for coral reef benthic communities, the number of observed species increases by less than 10% when the sampling scale is doubled. Similarly,

Bianchi et al. [63] points out the need for selecting a suitable sample size based on the dimensions of the organisms and the composition of the community and recognizes the fact that a priori standard reference sampling scales have not yet been defined. Other authors have shown that species richness is strongly dependent on sample size [80] and sampling quadrat densities [81–83], as well as indicating that comparing assemblages using different sample sizes may produce erroneous conclusions [84]. This is key for the interpretation of ancillary metrics, such as the Species Area Ratio (SAR) (i.e., the relationship between species richness and scale), which inform about the change in biodiversity in response to global environmental change [85].

Regarding Objective (3), results herein reported indicate that different sampling scales and quadrat densities should be considered when designing the sampling strategy depending on the metrics to be estimated. Special attention needs to be dedicated to the initial stages of the design of coral reef monitoring protocols with decisions being based on the metrics, as well as the type of statistical measures (i.e., central tendency or dispersion) being estimated. This should be coupled with the ecological relevance of these metrics and the spatio-temporal characteristics of the communities present within the sampling area. Failure to do so will result in biased estimates of the overall values.

Further work should focus on assessing the transferability of the framework presented here to other study areas. The shallow coral reef selected for the scope of the study is representative of the eastern South Africa coral reefs for this depth range [50,51,55,57], with the overall composition of the benthic community showing a preferential abundance for soft corals. These South African coral reefs are primarily characterized by soft coral communities growing on fossil dunes outcrops (i.e., Sodwana Bay) [47–49]. In particular, the site characterizes the Delagoa Bioregion, which constitutes the southernmost coral reef in the Western Indian Ocean [86]. These benthic communities have been monitored for the last 20 years along four fixed transects in Sodwana Bay (South Africa) [87] and have shown a shift in community composition due to changes in temperatures. The results herein presented are expected to be transferable to areas with similar characteristics and propose a sampling framework for wide-area (>1500 m<sup>2</sup>) coral reef characterization that contributes to overcoming some limitations in coral reef sampling. Based on the work by previous authors [49,57,87], the SfM methodology presented in this paper should be directly transferable to the coral reefs of KwaZulu-Natal province in Mozambique and the southern South African coral reefs, which present similar geomorphological characteristics [51].

This study quantifies the effect of sampling protocols on coral reef seascape metric estimation using high resolution underwater imagery coupled with the photogrammetry image processing technique for the case study area of Ponta do Ouro. A set of metrics derived from FRAGSTATS that inform about the overall quality of the coral reef area surveyed have been selected for the study. However, the framework can be expanded to assess the effect that sampling protocols have on other metrics (available or not within FRAGSTATS). For example, further work could explore the effect of sampling protocols on more classic metrics that are key for coral reef characterization (e.g., rugosity) or focus on the development of new metrics that can be derived from multiple geomatic products (e.g., point cloud, DEM and orthoimage). This will require the end user to develop scripts that can automatically derive the metrics within a GIS environment. The results herein presented are a step forward and contribute to improving current practice in coral reef monitoring protocols.

## 5. Conclusions

Current efforts on coral reef monitoring have focused on the estimation of the composition and health status. Seascape metrics can be also used to assess the quality of coral reefs. However, little effort has yet been dedicated to developing robust monitoring strategies for the accurate estimation of such metrics. This paper evaluates the effects that different sampling scales, quadrat density and sampling strategy have on seascape metric estimation when relying on SfM techniques. The SfM framework herein presented generates high resolution information that is useful for the characterization of the benthic communities down to single colonies. Results show that each of the seascape metrics considered in this study has different optimal sampling scales, quadrat densities and sampling strategies for

the case study area of Ponta do Ouro. Overall, sampling designs with over 30 (5 m × 5 m or 7 m × 7 m) quadrats provide representative results for most metrics considered here. Failure to select the appropriate monitoring strategy will result in biased estimates of these seascape metrics. The SfM framework has the potential to be transferred to similar coral reefs, specifically those of the KwaZulu-Natal province in Mozambique and the South African Republic. This paper contributes to improving current practice in high resolution coral reef monitoring protocols. The comparison of the metrics presented here with descriptive statistics limits the transferability of the outcomes to other coral reefs. Further work should focus on the validation of the proposed framework in other coral reefs. In addition, multiple sites need to be compared using a hierarchical modelling technique to account for a nested sampling design, with findings being used to determine the optimal sub-sampling area (quadrats) and intensity (number of quadrats) to accurately characterize this type of environment. This information would be very helpful in directing the design of future reef survey techniques.

**Acknowledgments:** This work was supported by the PhD scholarship “ EUREKA; European Social Funds (FSE), Programma Operativo Regionale (POR) 2014/2020 Regione Marche (Italy) ; the Marie Skłodowska-Curie Action, Horizon2020 within the project GreenBubbles (Grant Number 643712); the company UBICA srl. The authors would like to thank Miguel Goncalves, Director of Ponta do Ouro Partial Marine Reserve (Mozambique). Special thanks go to Jenny Stromvoll (Back to Basic Adventures Diving Center) for contributing to Figure 2. Thanks also to Dr. Fabrizio Torsani for his support in species identification. Thank you to Nicola Castelnovo as UBICA srl co-supervisor of my research. We thank four very helpful reviewers and the Editor for providing extremely useful comments, direction and constructive criticism. We will always be grateful.

**Author Contributions:** M.P. structured the research, designed and implemented the underwater sampling methodology. M.P. was in charge of implementing the photogrammetric process and digitization of sessile organisms. M.P. analyzed the data and implemented the sampling strategies considered in the manuscript. M.R.C. supervised the methodology and significantly contributed to structuring the manuscript. U.P. contributed to the development of the underwater sampling method. C.C. supervised the ecological aspects of the research. All authors read and approved the manuscript.

**Conflicts of Interest:** The authors declare no conflict of interest.

## References

- Hilmi, N.; Bambridge, T.; Claudet, J.; David, G.; Failler, P.; Feral, F.; Leopold, M.; Pascal, N.; Safa, A. Préserver la biodiversité des récifs coralliens: l'évaluation économique comme outil d'une gouvernance multi-échelle. In *Les Sciences Sociales dans le Pacifique Sud : Terrains, Questions et Méthodes*; Pacific-Credo Publications (Cahiers du Credo): Marseille, France, 2014; ISBN 978-2-9537485-2-9, pp. 291–312.
- Laurans, Y.; Pascal, N.; Binet, T.; Brander, L.; Clua, E.; David, G.; Rojat, D.; Seidl, A. Economic valuation of ecosystem services from coral reefs in the South Pacific: Taking stock of recent experience. *J. Environ. Manag.* **2013**, *116*, 135–144.
- Samonte, G.P.; Eisma-Osorio, R.L.; Amolo, R.; White, A. Economic value of a large marine ecosystem: Danajon double barrier reef, Philippines. *Ocean Coast. Manag.* **2016**, *122*, 9–19.
- Seenprachawong, U. An economic analysis of coral reefs in the Andaman Sea of Thailand. In *Marine and Coastal Ecosystem Valuation, Institutions, and Policy in Southeast Asia*; Springer: Singapore, 2016; pp. 31–45.
- Assessment, M.E. *Ecosystems and Human Well-Being*; World Resources Institute: Washington, DC, USA, 2003.
- Pascal, N.; Allenbach, M.; Brathwaite, A.; Burke, L.; Le Port, G.; Clua, E. Economic valuation of coral reef ecosystem service of coastal protection: A pragmatic approach. *Ecosyst. Serv.* **2016**, *21*, 72–80.
- Barbier, E.B.; Hacker, S.D.; Kennedy, C.; Koch, E.W.; Stier, A.C.; Silliman, B.R. The value of estuarine and coastal ecosystem services. *Ecol. Monogr.* **2011**, *81*, 169–193.
- Wilkinson, C.R.; Souter, D.N. *Status of Caribbean Coral Reefs after Bleaching and Hurricanes in 2005*; Global Coral Reef Monitoring Network: Townsville, Australia, 2008.
- Burke, L.; Reyntar, K.; Spalding, M.; Perry, A. *Reefs at Risk Revisited*; World Resources Institute: Washington, DC, USA, 2011.
- Mora, C. 36 Perpetual struggle for conservation in a crowded world and the needed paradigm shift for easing ultimate burdens. In *Ecology of Fishes on Coral Reefs*; Cambridge University Press: Cambridge, UK, 2015; Volume 20, p. 289.

11. Cheal, A.J.; MacNeil, M.A.; Emslie, M.J.; Sweatman, H. The threat to coral reefs from more intense cyclones under climate change. *Glob. Chang. Biol.* **2017**, *23*, 1511–1524.
12. The Government of the Hong Kong Special Administrative Region. Hong Kong Biodiversity Strategy Action Plan 2016–2021, 2016. Available online: [https://www.afcd.gov.hk/tc\\_chi/conservation/Con\\_hkbsap/files/HKBSAP\\_ENG\\_2.pdf](https://www.afcd.gov.hk/tc_chi/conservation/Con_hkbsap/files/HKBSAP_ENG_2.pdf) (accessed on 15 April 2017).
13. González-Rivero, M.; Beijbom, O.; Rodriguez-Ramirez, A.; Holtrop, T.; González-Marrero, Y.; Ganase, A.; Roelfsema, C.; Phinn, S.; Hoegh-Guldberg, O. Scaling up Ecological Measurements of Coral Reefs Using Semi-Automated Field Image Collection and Analysis. *Remote Sens.-Basel* **2016**, *8*, 30.
14. Hattori, A.; Shibuno, T. Total volume of 3D small patch reefs reflected in aerial photographs can predict total species richness of coral reef damselfish assemblages on a shallow back reef. *Ecol. Res.* **2015**, *30*, 675–682.
15. Hedley, J.D.; Roelfsema, C.M.; Chollett, I.; Harborne, A.R.; Heron, S.F.; Weeks, S.; Skirving, W.J.; Strong, A.E.; Eakin, C.M.; Christensen, T.R.; et al. Remote sensing of coral reefs for monitoring and management: A review. *Remote Sens.-Basel* **2016**, *8*, 118.
16. Beijbom, O.; Edmunds, P.J.; Kline, D.I.; Mitchell, B.G.; Kriegman, D. Automated annotation of coral reef survey images. In Proceedings of the 2012 IEEE Conference on Computer Vision and Pattern Recognition (CVPR), Providence Rhode Island Convention Center Providence, RI, USA, 16–21 June 2012; pp. 1170–1177.
17. Friedman, A.; Pizarro, O.; Williams, S.B.; Johnson-Roberson, M. Multi-scale measures of rugosity, slope and aspect from benthic stereo image reconstructions. *PLoS ONE* **2012**, *7*, e50440.
18. Williams, S.B.; Pizarro, O.R.; Jakuba, M.V.; Johnson, C.R.; Barrett, N.S.; Babcock, R.C.; Kendrick, G.A.; Steinberg, P.D.; Heyward, A.J.; Doherty, P.J.; et al. Monitoring of benthic reference sites: using an autonomous underwater vehicle. *IEEE Robot. Autom. Mag.* **2012**, *19*, 73–84.
19. Ferrari, R.; Bryson, M.; Bridge, T.; Hustache, J.; Williams, S.B.; Byrne, M.; Figueira, W. Quantifying the response of structural complexity and community composition to environmental change in marine communities. *Glob. Chang. Biol.* **2016**, *22*, 1965–1975.
20. Costa, B.; Battista, T.; Pittman, S. Comparative evaluation of airborne LiDAR and ship-based multibeam SoNAR bathymetry and intensity for mapping coral reef ecosystems. *Remote Sens. Environ.* **2009**, *113*, 1082–1100.
21. De'ath, G.; Fabricius, K.E.; Sweatman, H.; Puotinen, M. The 27-year decline of coral cover on the Great Barrier Reef and its causes. *Proc. Natl. Acad. Sci. USA* **2012**, *109*, 17995–17999.
22. Zhang, C.; Selch, D.; Xie, Z.; Roberts, C.; Cooper, H.; Chen, G. Object-based benthic habitat mapping in the Florida Keys from hyperspectral imagery. *Estuar. Coast. Shelf Sci.* **2013**, *134*, 88–97.
23. Barnes, B.B.; Hallock, P.; Hu, C.; Muller-Karger, F.; Palandro, D.; Walter, C.; Zepp, R. Prediction of coral bleaching in the Florida Keys using remotely sensed data. *Coral Reefs* **2015**, *34*, 491–503.
24. Lecours, V.; Devillers, R.; Schneider, D.C.; Lucieer, V.L.; Brown, C.J.; Edinger, E.N. Spatial scale and geographic context in benthic habitat mapping: Review and future directions. *Mar. Ecol. Prog. Ser.* **2015**, *535*, 259–284.
25. Leon, J.X.; Roelfsema, C.M.; Saunders, M.I.; Phinn, S.R. Measuring coral reef terrain roughness using 'Structure-from-Motion' close-range photogrammetry. *Geomorphology* **2015**, *242*, 21–28.
26. Storlazzi, C.D.; Dartnell, P.; Hatcher, G.A.; Gibbs, A.E. End of the chain? Rugosity and fine-scale bathymetry from existing underwater digital imagery using structure-from-motion (SfM) technology. *Coral Reefs* **2016**, *35*, 889–894.
27. Figueira, W.; Ferrari, R.; Weatherby, E.; Porter, A.; Hawes, S.; Byrne, M. Accuracy and precision of habitat structural complexity metrics derived from underwater photogrammetry. *Remote Sens.-Basel* **2015**, *7*, 16883–16900.
28. Carrivick, J.L.; Smith, M.W.; Quincey, D.J. *Structure from Motion in the Geosciences*; John Wiley & Sons: Hoboken, NJ, USA, 2016.
29. Westoby, M.; Brasington, J.; Glasser, N.; Hambrey, M.; Reynolds, J. 'Structure-from-Motion' photogrammetry: A low-cost, effective tool for geoscience applications. *Geomorphology* **2012**, *179*, 300–314.
30. McCarthy, J.; Benjamin, J. Multi-image photogrammetry for underwater archaeological site recording: An accessible, diver-based approach. *J. Marit. Archaeol.* **2014**, *9*, 95–114.
31. Casella, E.; Collin, A.; Harris, D.; Ferse, S.; Bejarano, S.; Parravicini, V.; Hench, J.L.; Rovere, A. Mapping coral reefs using consumer-grade drones and structure from motion photogrammetry techniques. *Coral Reefs* **2016**, *1*, 269–275.

32. González-Rivero, M.; Bongaerts, P.; Beijbom, O.; Pizarro, O.; Friedman, A.; Rodríguez-Ramírez, A.; Upcroft, B.; Laffoley, D.; Kline, D.; Bailhache, C.; et al. The Catlin Seaview Survey—kilometre-scale seascape assessment, and monitoring of coral reef ecosystems. *Aquat. Conserv.* **2014**, *24*, 184–198.
33. Burns, J.; Delparte, D.; Kapon, L.; Belt, M.; Gates, R.; Takabayashi, M. Assessing the impact of acute disturbances on the structure and composition of a coral community using innovative 3D reconstruction techniques. *Method Oceanogr.* **2016**, *15*, 49–59.
34. Chirayath, V.; Earle, S.A. Drones that see through waves—preliminary results from airborne fluid lensing for centimetre-scale aquatic conservation. *Aquat. Conserv.: Mar. Freshw. Ecosyst.* **2016**, *26*, 237–250.
35. Gutiérrez-Heredia, L.; D’Helft, C.; Reynaud, E. Simple methods for interactive 3D modeling, measurements, and digital databases of coral skeletons. *Limnol. Oceanogr.: Methods* **2015**, *13*, 178–193.
36. Lavy, A.; Eyal, G.; Neal, B.; Keren, R.; Loya, Y.; Ilan, M. A quick, easy and non-intrusive method for underwater volume and surface area evaluation of benthic organisms by 3D computer modelling. *Methods Ecol. Evol.* **2015**, *6*, 521–531.
37. Boström, C.; Pittman, S.J.; Simenstad, C.; Kneib, R.T. Seascape ecology of coastal biogenic habitats: Advances, gaps, and challenges. *Mar. Ecol. Prog. Ser.* **2011**, *427*, 191–217.
38. Wedding, L.M.; Lepczyk, C.A.; Pittman, S.J.; Friedlander, A.M.; Jorgensen, S. Quantifying seascape structure: Extending terrestrial spatial pattern metrics to the marine realm. *Mar. Ecol. Prog. Ser.* **2011**, *427*, 219–232.
39. Kendall, M.S.; Miller, T. The influence of thematic and spatial resolution on maps of a coral reef ecosystem. *Mar. Geod.* **2008**, *31*, 75–102.
40. Garrabou, J.; Riera, J.; Zabala, M. Landscape pattern indices applied to Mediterranean subtidal rocky benthic communities. *Landsc. Ecol.* **1998**, *13*, 225–247.
41. Garrabou, J.; Ballesteros, E.; Zabala, M. Structure and dynamics of north-western Mediterranean rocky benthic communities along a depth gradient. *Estuar. Coast. Shelf Sci.* **2002**, *55*, 493–508.
42. Turner, M.G. Landscape Ecol: The effect of pattern on process. *Annu. Rev. Ecol. Syst.* **1989**, *20*, 171–197.
43. Pittman, S.J.; Costa, B.M.; Battista, T.A. Using lidar bathymetry and boosted regression trees to predict the diversity and abundance of fish and corals. *J. Coast. Res.* **2009**, doi:10.2112/SI53-004.1.
44. Wedding, L.M.; Friedlander, A.M.; McGranaghan, M.; Yost, R.S.; Monaco, M.E. Using bathymetric lidar to define nearshore benthic habitat complexity: Implications for management of reef fish assemblages in Hawaii. *Remote Sens. Environ.* **2008**, *112*, 4159–4165.
45. Purkis, S.J.; Graham, N.; Riegl, B. Predictability of reef fish diversity and abundance using remote sensing data in Diego Garcia (Chagos Archipelago). *Coral Reefs* **2008**, *27*, 167–178.
46. Schleyer, M. South African coral communities. In *Coral Reefs of the Indian Ocean: Their Ecology and Conservation*; Oxford University Press: New York, NY, USA, 2000; pp. 83–105.
47. Ramsay, P. Marine geology of the Sodwana Bay shelf, southeast Africa. *Mar. Geol.* **1994**, *120*, 225–247.
48. Ramsay, P. Quaternary marine geology of the Sodwana Bay continental shelf, Northern KwaZulu-Natal. *Oceanogr. Lit. Rev.* **1996**, *11*, 1103.
49. Schleyer, M.; Celliers, L. Coral dominance at the reef–sediment interface in marginal coral communities at Sodwana Bay, South Africa. *Mar. Freshw. Res.* **2004**, *54*, 967–972.
50. Riegl, B. Taxonomy and Ecology of South African Reef Corals. Ph.D. Thesis, University of Cape Town, Cape Town, South Africa, 1993.
51. Jordan, I.E.; Samways, M.J. Recent changes in coral assemblages of a South African coral reef, with recommendations for long-term monitoring. *Biodivers. Conserv.* **2001**, *10*, 1027–1037.
52. Celliers, L.; Schleyer, M.H. Coral community structure and risk assessment of high-latitude reefs at Sodwana Bay, South Africa. *Biodivers. Conserv.* **2008**, *17*, 3097–3117.
53. Robertson, W.; Schleyer, M.; Fielding, P.; Tomalin, B.; Beckley, L.; Fennessy, S.; Van der Elst, R.; Bandeira, S.; Macia, A.; Gove, D. *Inshore Marine Resources and Associated Opportunities for Development of the Coast of Southern Mozambique: Ponta do Ouro to Cabo de Santa Maria*; Technical report; Oceanographic Research Institute: Durban, South Africa, 1996; Unpublished report.
54. Dai, C.F. Interspecific competition in Taiwanese corals with special reference to interactions between alcyonaceans and scleractinians. *Mar. Ecol. Prog. Ser.* **1990**, *60*, 291–297.
55. Riegl, B. Effects of sand deposition on scleractinian and alcyonacean corals. *Mar. Biol.* **1995**, *121*, 517–526.

56. Schumann, E.; Orren, M. *The Physico-Chemical Characteristics of the South-West Indian Ocean in Relation to Maputaland*; Rhodes University: Grahamstown, South Africa; The Wildlife Society of Southern Africa: Durban, South Africa, 1980; pp. 8–11.
57. Schleyer, M.H.; Kruger, A.; Celliers, L. Long-term community changes on a high-latitude coral reef in the Greater St Lucia Wetland Park, South Africa. *Mar. Pollut. Bull.* **2008**, *56*, 493–502.
58. Ferraris, D.; Palma, M.; Pantaleo, U.; Cerrano, C.; Chiantore, M. Method and Device for Tracking the Path of an Object. PCT/IB2016/053924, 9 March 2017.
59. Roelfsema, C.; Phinn, S.; Jupiter, S.; Comley, J.; Albert, S. Mapping coral reefs at reef to reef-system scales, 10s–1000s km<sup>2</sup>, using object-based image analysis. *Int. J. Remote Sens.* **2013**, *34*, 6367–6388.
60. Edinger, E.N.; Risk, M.J. Reef classification by coral morphology predicts coral reef conservation value. *Biol. Conserv.* **2000**, *92*, 1–13.
61. MacArthur, R.H.; Wilson, E.O. *Theory of Island Biogeography*. (MPB-1); Princeton University Press: Princeton, NJ, USA, 2015; Volume 1.
62. Weinberg, S. A comparison of coral reef survey methods. *Bijdragen tot de Dierkunde* **1981**, *51*, 199–218.
63. Bianchi, C.; Pronzato, R.; Cattaneo-Vietti, R.; Benedetti-Cecchi, L.; Morri, C.; Pansini, M.; Chemello, R.; Milazzo, M.; Frascchetti, S.; Terlizzi, A.; et al. Hard bottoms. *Biol. Mar. Mediterr.* **2004**, *11*, 185–215.
64. Guinda, X.; Gracia, A.; Puente, A.; Juanes, J.A.; Rzhhanov, Y.; Mayer, L. Application of landscape mosaics for the assessment of subtidal macroalgae communities using the CFR index. *Deep Sea Res. II: Top. Stud. Oceanogr.* **2014**, *106*, 207–215.
65. Mcgarigal, K.; Cushman, S.A.; Neel, M.C.; Ene, E. *FRAGSTATS: Spatial Pattern Analysis Program for Categorical Maps*; Technical report; Department of Environmental Conservation University of Massachusetts: Amherst, MA, USA, 2002.
66. Teixido, N.; Garrabou, J.; Arntz, W. Spatial pattern quantification of Antarctic benthic communities using landscape indices. *Mar. Ecol. Prog. Ser.* **2002**, *242*, 1–14.
67. McGarigal, K.; Marks, B.J. *FRAGSTATS: Spatial Pattern Analysis Program for Quantifying Landscape Structure*; Gen tech rep pnw-gtr-351; United States Department of Agriculture, Forest Service, Pacific Northwest Research Station: Corvallis, OR, USA, 1995.
68. Dornelas, M.; Madin, J.S.; Baird, A.H.; Connolly, S.R. Allometric growth in reef-building corals. *Proc. R. Soc. B Biol. Sci.* **2017**, *284*. Available online: <http://rspb.royalsocietypublishing.org/content/284/1851/20170053.full.pdf> (accessed on 1 May 2017).
69. He, H.S.; DeZonia, B.E.; Mladenoff, D.J. An aggregation index (AI) to quantify spatial patterns of landscapes. *Landsc. Ecol.* **2000**, *15*, 591–601.
70. Cowen, R.K.; Sponaugle, S. Larval dispersal and marine population connectivity. *Annu. Rev. Mar. Sci.* **2009**, *1*, 443–466.
71. Nyström, M. Redundancy and response diversity of functional groups: Implications for the resilience of coral reefs. *AMBIO: J. Hum. Environ.* **2006**, *35*, 30–35.
72. Spellerberg, I.F.; Fedor, P.J. A tribute to Claude Shannon (1916–2001) and a plea for more rigorous use of species richness, species diversity and the ‘Shannon–Wiener’ Index. *Glob. Ecol. Biogeogr.* **2003**, *12*, 177–179.
73. Somerfield, P.; Clarke, K.; Warwick, R. Simpson index. In *Encyclopedia of Ecology*; Elsevier: Amsterdam, The Netherlands, 2008.
74. Hawkins, S.; Hartnoll, R. A study of the small-scale relationship between species number and area on a rocky shore. *Estuar. Coast. Mar. Sci.* **1980**, *10*, 201–214.
75. Sleeman, J.C.; Kendrick, G.A.; Boggs, G.S.; Hegge, B.J. Measuring fragmentation of seagrass landscapes: Which indices are most appropriate for detecting change? *Mar. Freshw. Res.* **2005**, *56*, 851–864.
76. Starmans, A.; Gutt, J. Mega-epibenthic diversity: A polar comparison. *Mar. Ecol. Prog. Ser.* **2002**, *225*, 45–52.
77. Starmans, A.; Gutt, J.; Arntz, W. Mega-epibenthic communities in Arctic and Antarctic shelf areas. *Mar. Biol.* **1999**, *135*, 269–280.
78. Floros, C.; Schleyer, M. The functional importance of *Acropora austera* as nursery areas for juvenile reef fish on South African coral reefs. *Coral Reefs* **2016**, *1*, 139–149.
79. Weinberg, S. The minimal area problem in invertebrate communities of Mediterranean rocky substrata. *Mar. Biol.* **1978**, *49*, 33–40.
80. Drakare, S.; Lennon, J.J.; Hillebrand, H. The imprint of the geographical, evolutionary and ecological context on species–area relationships. *Ecol. Lett.* **2006**, *9*, 215–227.

81. Walther, B.A.; Martin, J.L. Species richness estimation of bird communities: How to control for sampling effort? *IBIS* **2001**, *143*, 413–419.
82. Condit, R.; Hubbell, S.P.; Lafrankie, J.V.; Sukumar, R.; Manokaran, N.; Foster, R.B.; Ashton, P.S. Species-area and species-individual relationships for tropical trees: A comparison of three 50-ha plots. *J. Ecol.* **1996**, *84*, 549–562.
83. Gotelli, N.J.; Colwell, R.K. Quantifying biodiversity: procedures and pitfalls in the measurement and comparison of species richness. *Ecol. Lett.* **2001**, *4*, 379–391.
84. Stout, J.; Vandermeer, J. Comparison of species richness for stream-inhabiting insects in tropical and mid-latitude streams. *Am. Nat.* **1975**, *109*, 263–280.
85. Thomas, C.D.; Cameron, A.; Green, R.E.; Bakkenes, M.; Beaumont, L.J.; Collingham, Y.C.; Erasmus, B.F.; De Siqueira, M.F.; Grainger, A.; Hannah, L.; et al. Extinction risk from climate change. *Nature* **2004**, *427*, 145–148.
86. Porter, S.; Branch, G.; Sink, K. Biogeographic patterns on shallow subtidal reefs in the western Indian Ocean. *Mar. Biol.* **2013**, *160*, 1271–1283.
87. Porter, S.; Schleyer, M. Long-term dynamics of a high-latitude coral reef community at Sodwana Bay, South Africa. *Coral Reefs* **2017**, *36*, 369–382.



© 2017 by the authors. Licensee MDPI, Basel, Switzerland. This article is an open access article distributed under the terms and conditions of the Creative Commons Attribution (CC BY) license (<http://creativecommons.org/licenses/by/4.0/>).

# High resolution orthomosaics of African coral reefs: a tool for wide-scale benthic monitoring

Palma, Marco

2017-07-08

Attribution 4.0 International

---

M. Palma, M. Rivas Casado, U. Pantaleo, C. Cerrano. High resolution orthomosaics of African coral reefs: a tool for wide-scale benthic monitoring. *Remote Sensing*, 2017, Vol.9, Iss.7, article number 705

<http://dx.doi.org/10.3390/rs9070705>

*Downloaded from CERES Research Repository, Cranfield University*